

Electroreflectance spectroscopy of strained $\text{Si}_{1-x}\text{Ge}_x$ layers on silicon

T. Ebner, K. Thonke, and R. Sauer

Abteilung Halbleiterphysik, Universität Ulm, 89069 Ulm, Germany

F. Schaeffler and H. J. Herzog

Daimler-Benz-Forschungsinstitut, Wilhelm-Runge-Strasse 11, 89081 Ulm, Germany

(Received 26 November 1997)

Electroreflectance spectroscopy was used to measure the critical point energies in strained $\text{Si}_{1-x}\text{Ge}_x$ layers on Si in the energy region from 3 to 6 eV. Observed were the transitions $E_1, E_1 + \Delta_1, E'_0, E_0, E_0 + \Delta_0, E_2(X), E_2(\Sigma)$, and E'_1 for germanium concentrations ranging from 12.5% to 28.1% at sample temperatures between 10 and 300 K. The transitions $E_1 + \Delta_1, E_0, E_0 + \Delta_0, E_2(\Sigma)$, and E'_1 and their temperature dependence have not been reported before in strained $\text{Si}_{1-x}\text{Ge}_x$ layers. Calculations of the strain shifts based on deformation potential theory are in good agreement with the experimental shifts of the E_0 transition, while deviations occur for the E_1 transition. [S0163-1829(98)12319-6]

I. INTRODUCTION

Strained $\text{Si}_{1-x}\text{Ge}_x$ layers grown epitaxially on silicon were intensely studied during the last years. Several devices, e.g., high frequency bipolar transistors based on SiGe heterostructures, are already in use, and infrared detectors in the 4- μm range are being developed. Such hopes have motivated investigations of the fundamental indirect band gap of SiGe/Si heterostructures in a wide range of Ge concentrations and of several direct gaps in $\text{Si}_{1-x}\text{Ge}_x$ superlattices. However, much less information is available on the direct gaps in single $\text{Si}_{1-x}\text{Ge}_x$ layers on Si. The aim of our work is to investigate the dependence of direct optical transitions on the germanium concentration x in strained $\text{Si}_{1-x}\text{Ge}_x$ layers. It appeared desirable to separate the influences of composition and strain, hence we restricted ourselves to the study of thick single strained layers, thus avoiding the complications of folded band structures associated with superlattices. In this work we present our investigations of a series of pseudomorphic $\text{Si}_{1-x}\text{Ge}_x$ films with germanium concentrations between 12.5% and 28% by electroreflectance (ER) spectroscopy in the energy range from 3 to 6 eV and for temperatures between 10 and 300 K. We derive transition energies for the major critical points $E_0, E'_0, E_1, E_2, E'_1$ and their split-off companions, and discuss deformation potential values.

II. EXPERIMENT

All samples were grown at the Daimler Benz Research Institute in Ulm by molecular beam epitaxy (MBE). A silicon buffer layer was first grown on the (001) silicon substrate followed by a 300 Å fully strained epilayer of $\text{Si}_{1-x}\text{Ge}_x$ and a 50-Å-thick cap layer of silicon. The thickness of the $\text{Si}_{1-x}\text{Ge}_x$ layer was smaller than the critical thickness, but large enough to keep energy shifts of the electron and hole states due to quantum confinement below measurable limits. The germanium concentrations were determined by photoluminescence measurements in addition to estimates from the growth, and were found to be between 12.5% and 28.1% (Table I). The n -type samples were con-

tacted using 5-nm-thick Au Schottky barriers on top and 200-nm Ti contacts on the substrate side. The p -type samples received semitransparent 5-nm-thick Ti top contacts and 200-nm Al substrate contacts. A modulated electric field in the sample was created by applying a sine voltage at a frequency of 225 Hz. The beam probing the reflectivity of the samples was either from a 75-W Xe arc lamp or from a 50-W deuterium lamp (for short wavelengths) dispersed by a monochromator of 0.25-m focal length. All measurements were performed within the low-field limit. The ER spectra were analyzed using the typical third derivative line shape¹

$$\frac{\Delta R}{R} = \text{Re}[A e^{i\theta} (E - E_g + i\Gamma)^{-n}], \quad (1)$$

where A is the signal amplitude, Γ the line broadening, E_g the energy of the investigated critical point in the combined density of states, and E the incident photon energy. θ is a phase factor and n varies between 2.5 and 4, depending on the type of the critical point. We have used both p - and n -type samples to investigate different types of contacts. There should be no essential physical difference in the investigated optical transitions for different doping. However, the phase factor θ can change between p - and n -type samples and therefore allows for an independent check of the reliability of our fit parameters at critical points derived. For most samples we obtained a better signal-to-noise ratio for p -type samples.

III. THEORETICAL CALCULATION OF THE TRANSITION ENERGIES

The band structures of silicon and germanium are shown in Fig. 1 indicating the optical transitions $E'_1, E_1, E'_0, E_0, E_2(X)$, and $E_2(\Sigma)$, which are studied in the following. All corresponding transitions with the participation of split-off valence and conduction bands were omitted for clarity. Kline, Pollak, and Cardona¹⁶ have shown experimentally that the transition energies $h\nu$ for $E_0, E_0 + \Delta_0, E_1, E_1 + \Delta_1, E'_0, E'_0 + \Delta'_0$, and E_2 in unstrained

TABLE I. Literature data of parameters in Si and Ge relevant for the present investigation: Deformation potentials a and b , elastic moduli c_{11} and c_{12} , transition energies and split-off energies Δ_0 for the E_0 transition (Refs. 2–8), Varshni parameters for the E'_0 transition (Refs. 9,10), deformation potentials, transition energies and split-off energies of the E_1 transition (Refs. 8,11,12–14).

	a (eV)	b (eV)	$c_{11}[10^6 \text{ (N/cm}^2\text{)}]$	$c_{12}[10^6 \text{ (N/cm}^2\text{)}]$	E_0 (meV)	Δ_0 (meV)
Si	-12.4	-2.2	16.772	6.498	4175	44
Ge	-8.6	-3.0	13.112	4.923	882	296
	$\alpha(10^{-4} \text{ eV/K})$	β (K)	D_1^1 (eV)	D_3^3 (eV)	E_1 (meV)	Δ_1 (meV)
Si	5.37	342	-8	5	3452	29
Ge	3.6	344	-8.2	5.8	2239	184

$\text{Si}_{1-x}\text{Ge}_x$ bulk alloys can be well described as linear interpolations between the known values of silicon and germanium

$$h\nu_{\text{Si}_{1-x}\text{Ge}_x} = E_{g,\text{Si}_{1-x}\text{Ge}_x} = xE_{g,\text{Ge}} + (1-x)E_{g,\text{Si}}. \quad (2)$$

The strain present in our pseudomorphically grown SiGe alloy layers modifies these transition energies as discussed below.

For clarity, we summarize here briefly the formulas and parameters used in our derivation of deformation potentials. When $\text{Si}_{1-x}\text{Ge}_x$ layers are grown epitaxially on (001) silicon, lattice mismatch causes a biaxial compressive strain

$$\epsilon_{xx} = \epsilon_{yy} = \epsilon = -0.0418x \quad (3)$$

along the [100] and [010] directions and a uniaxial tensile strain

$$\epsilon_{zz} = -K\epsilon = -\frac{2c_{12}}{c_{11}}\epsilon \quad (4)$$

along the [001] axis, where c_{11} and c_{12} are the cubic elastic moduli. The stress tensor can be split into a uniaxial and a hydrostatic part, the former inducing shifts and splittings and the latter inducing only shifts of the transition energies.

The E_0 transition occurs between the points $\Gamma_{25'}$ of the valence band (VB) and $\Gamma_{2'}$ of the conduction band (CB). In unstrained material the VB at the Γ point consists of the twofold degenerate split-off band (so band) and the fourfold degenerate band. The latter is split under uniaxial stress into twofold degenerate light (lh) and heavy-hole (hh) bands. Hence, there are three possible E_0 transitions to the unsplit $\Gamma_{2'}$ CB labeled $E_0(1)$ (hh band), $E_0(2)$ (lh band), and $E_0(3)$ (so band). The transition energies in strained material can be calculated as a function of the germanium concentration as^{11,17}

$$\begin{aligned} E_0(1) &= E_0 + E_H + E_S, \\ E_0(2) &= E_0 + E_H - \frac{E_S}{2} + \frac{\Delta_0}{2} - \frac{1}{2}\sqrt{\Delta_0^2 + 2\Delta_0 E_S + 9E_S^2}, \\ E_0(3) &= E_0 + E_H - \frac{E_S}{2} + \frac{\Delta_0}{2} + \frac{1}{2}\sqrt{\Delta_0^2 + 2\Delta_0 E_S + 9E_S^2}, \end{aligned} \quad (5)$$

where E_0 is the transition energy of the unstrained material, Δ_0 the spin-orbit splitting energy at the $\Gamma_{25'}$ point, and $E_H = a(2-K)\epsilon$ and $E_S = -b(1+K)\epsilon$ are matrix elements due to the hydrostatic and uniaxial stress, respectively. Here, a denotes the hydrostatic interband deformation potential (i.e., a describes the relative shift of the CB and VB), and b is the tetragonal deformation potential of the valence band. The constants a , b , c_{11} , c_{12} , E_0 , and Δ_0 are known for silicon and germanium and can be calculated for $\text{Si}_{1-x}\text{Ge}_x$ by linear interpolation. The values for silicon and germanium at 70 K are specified in Table I, and the calculated transition energies are shown in Fig. 2. Obviously, theory predicts a decrease of the energy of all three E_0 transitions with increasing germanium content.

Next we consider the E'_0 transition occurring between the $\Gamma_{25'}$ VB and the Γ_{15} CB. There are no theoretical calculations for the change of the Γ_{15} CB under biaxial stress, but there is a photoreflectance measurement by Yin *et al.*¹⁸ at 300 K for germanium concentrations up to 23%. Linear interpolation of the latter data set yields the transition energy for the strained alloy

$$E_g(x) = (3331 - 225x) \text{ meV}. \quad (6)$$

The 300-K transition energy can approximately be extrapolated to 70 K by interpolating linearly the parameters of the Varshni formula¹⁹ for $\text{Si}_{1-x}\text{Ge}_x$ between the values of silicon and germanium. The required data are listed in Table I. Since Yin *et al.*¹⁸ experimentally resolved only one transition, it is reasonable to assign it to a superposition of the transitions $E'_0(1)$ and $E'_0(2)$ with an observed average transition energy. Thus, with the known splitting between the E_0 subtransitions (reflecting the splitting of the $\Gamma_{25'}$ VB) the energies for the three corresponding E'_0 transitions can be calculated, taking into account the strain shifts of the $\Gamma_{25'}$ VB. The results are shown in Fig. 2. It is not clear to which CB the transition measured by Yin *et al.* belongs, since the Γ_{15} CB has degeneracy properties similar to the $\Gamma_{25'}$ VB: it consists of a fourfold degenerate and a twofold degenerate band in unstrained material, and of three twofold degenerate bands in strained $\text{Si}_{1-x}\text{Ge}_x$. In germanium, the Γ_{15} CB split-off energy amounts to 200 meV and both transitions, E'_0 and $E'_0 + \Delta'_0$, have the same transition strength. Unfortunately, there are no data for silicon in the literature.

The E_1 transition occurs between the Λ_3 dispersion branch of the VB and the Λ_1 dispersion branch of the CB. The transition energies can be calculated as^{11,17}

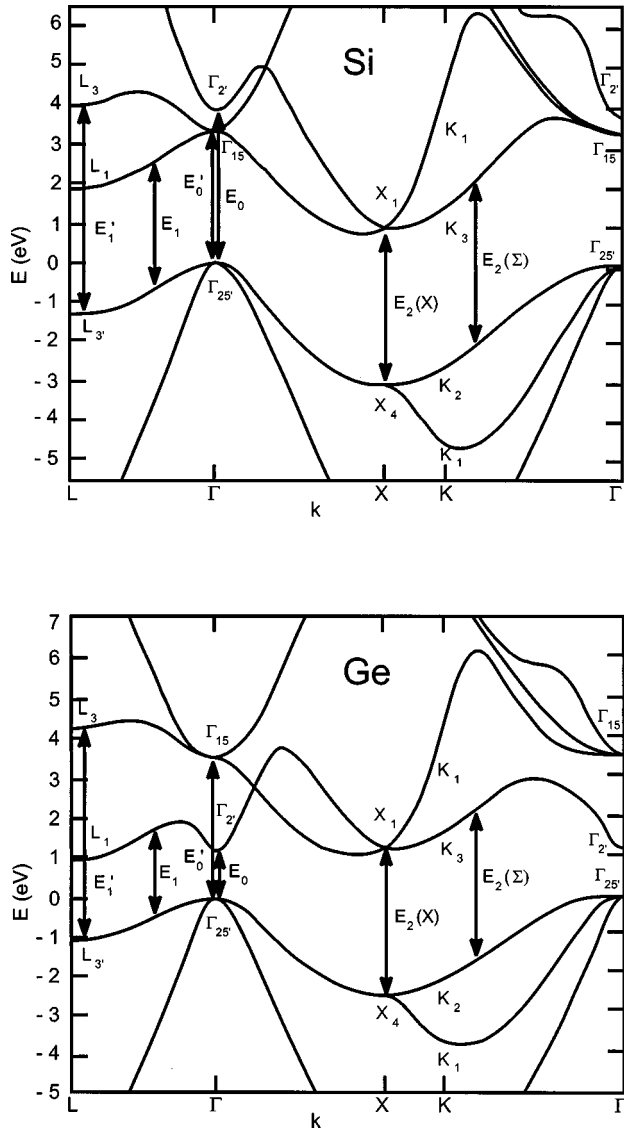


FIG. 1. Band structure of silicon and germanium following Ref. 15 with transitions labeled.

$$E_1(\epsilon) = E_1 + \frac{1}{2}\Delta_1 + \delta_H - \sqrt{\left(\frac{1}{2}\Delta_1\right)^2 + (\delta_J \pm \delta_S)^2},$$

$$(E_1 + \Delta_1)(\epsilon) = E_1 + \frac{1}{2}\Delta_1 + \delta_H + \sqrt{\left(\frac{1}{2}\Delta_1\right)^2 + (\delta_J \pm \delta_S)^2}, \quad (7)$$

where $\delta_H = (D_1^1/\sqrt{3})(2-K)\epsilon$ and $\delta_S = \sqrt{\frac{2}{3}}D_3^3(1+K)\epsilon$ are matrix elements due to the hydrostatic and uniaxial parts of the stress, respectively. The matrix element δ_J describing the electron-hole exchange interaction can be neglected¹¹ and the interband deformation potentials D_1^1, D_3^3 , the split-off energy Δ_1 , and the transition energies E_1 and $E_1 + \Delta_1$ in unstrained material were taken as linear interpolations between germanium and silicon. The values of silicon and germanium used here are specified in Table I. The calculated energies for strained material are shown in Fig. 2 as a function of the germanium concentration. The strain causes a negligible additional shift for the E_1 transition, since the hydrostatic and uniaxial parts of the strain compensate each other, while there is an evident strain shift of the $E_1 + \Delta_1$ transition.

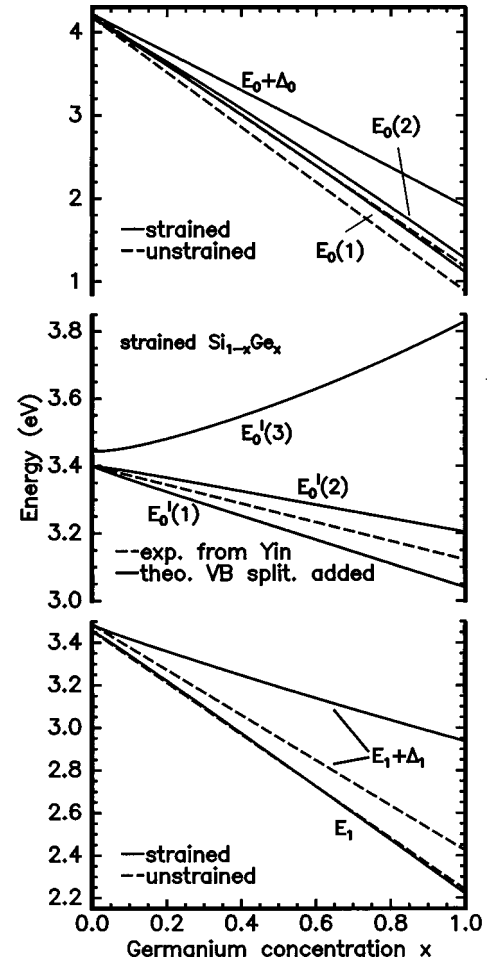


FIG. 2. Theoretically calculated transition energies in strained $\text{Si}_{1-x}\text{Ge}_x$ at 70 K. Top: Linear interpolation of E_0 transition energies (dashed lines) and calculated energies in strained material (solid lines). Middle: Linearly interpolated E_0' transition energies from Yin (Ref. 18) for strained $\text{Si}_{1-x}\text{Ge}_x$ converted to 70 K (dashed line), and calculated strain splitting caused by the splitting of the $\Gamma_{25'}$ VB (solid lines). The unknown splitting of the Γ_{15} CB is neglected. Bottom: Linear interpolation of E_1 transition energies (solid lines) and calculated transition energies in strained material (dashed lines). Data from Table I.

IV. EXPERIMENTAL RESULTS AND DISCUSSION

Experimental results on the two series of samples obtained at 70 K are shown in Figs. 3 and 4. The dominant structure in all spectra is due to the transitions E_1 and E_0' . The E_0' transition, which is very weak in germanium and also weaker than the E_1 transition in pure silicon, yields the highest peak in strained $\text{Si}_{1-x}\text{Ge}_x$. The transition E_0 —in germanium as strong as the E_1 transition—is relatively weak for small germanium concentrations and cannot be resolved in all of the spectra. The structures due to the E_2 and E_1' transitions are complex and can be explained solely by assuming a superposition of several critical points. However, there is only a weak dependence of these transitions on the germanium concentration. Around 3 eV in Fig. 4 the onset of strong oscillations is visible, which extend to lower energies. They emerge mainly for n -type samples and originate from interferences due to multiple reflections in the samples²⁰.

The results for the E_1 transition are summarized in Fig. 5.

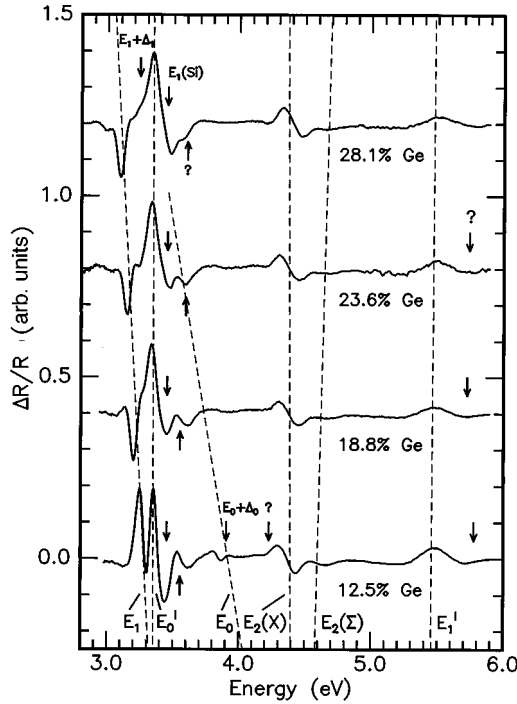


FIG. 3. Measured electroreflectance spectra of p -type samples at 70 K. Dashed lines and arrows indicate the various band gaps as a function of the Ge content x as obtained from fits to the experimental data. Unidentified transitions are denoted by question marks.

To fit the experimental spectra we have used $n=3$ in Eq. (1) for a two-dimensional critical point. A linear interpolation of the measured transition energies, using the E_1 transition energy for pure Si, as a known fix point, yields

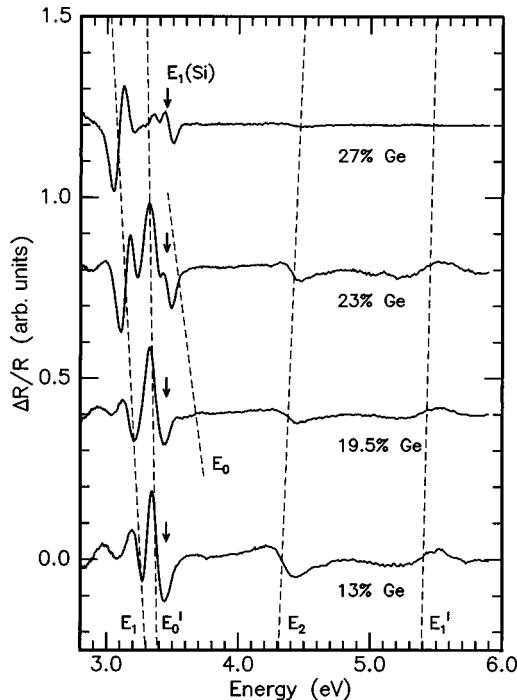


FIG. 4. Measured electroreflectance spectra of n -type samples at 70 K. Dashed lines and arrows indicate the various band gaps as a function of the Ge content x as obtained from fits to the experimental data. Unidentified transitions are denoted by question marks.

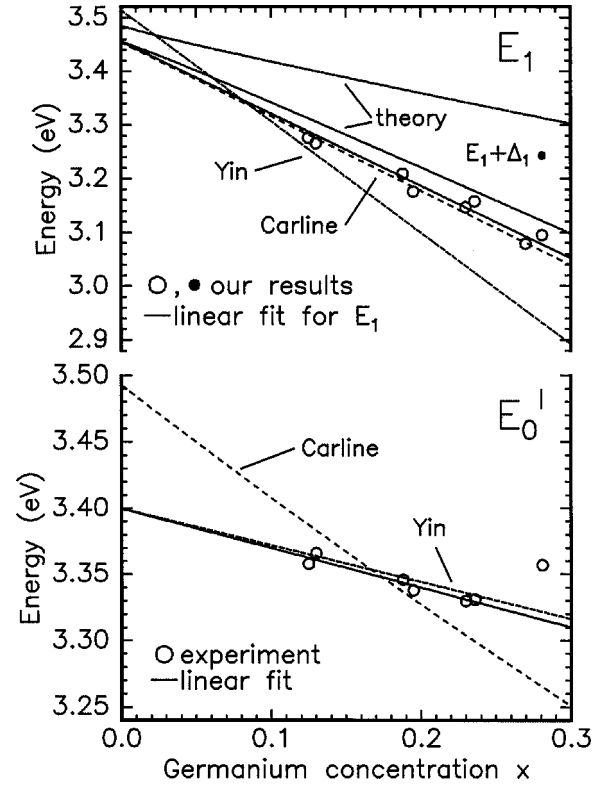


FIG. 5. Experimental ER results of strained $\text{Si}_{1-x}\text{Ge}_x$ at 70 K for transitions E_1 and E'_0 . The data of the E_1 transition were linearly fitted including the energy 3.45 eV for pure silicon, $x=0$. Included for comparison are data of other work by Yin, Ref. 18 and Carline, Ref. 21.

$$E_1(x) = [3452 - (1345 \pm 25)x] \text{ meV}. \quad (8)$$

The $E_1 + \Delta_1$ transition involving the spin-orbit splitting Δ_1 could be resolved only for one sample, since it is obscured by the E'_0 transition. Referring to the E_1 transition, all data available in the literature were measured at 300 K. From these data we estimate the 70-K values by interpolating the parameters in the Varshni equation linearly between silicon and germanium. Our measurements are in good agreement with extrapolated data taken from ellipsometry measurements of Carline *et al.*,²¹ but they definitely deviate from those given by Yin *et al.*¹⁸ This is not surprising, since already the extrapolation from Yin's measurement for $x=0$ does not agree with measurements of pure silicon. The agreement with our theoretical calculations is even worse. We have tried to fit the interpolating expression to our measurement by varying the deformation potentials and obtain $D_1^1 = -2$ eV and $D_3^3 = 4$ eV. The absolute value of the hydrostatic deformation potential D_1^1 derived in this way is unacceptably small when compared to the literature value $D_1^1 = -8$ eV. At present, this discrepancy can only be traced back to inaccuracies in the fit caused by the near by E'_0 transition and to the fact that we have experimental data only for samples up to 28.1% germanium concentration.

The dependence of the E'_0 transition on the germanium concentration is relatively weak (see Fig. 5). The fits were made under the assumption of a three-dimensional critical point ($n=2.5$). Here our measurements are in good agreement with Yin *et al.*'s data, while they deviate from Carline

et al.'s data. Like Yin *et al.*'s measurements for the E_1 transition, the extrapolation from Carline's measurements for $x=0$ does not agree with the transition energies of pure silicon in the literature. It is remarkable that the linewidth of the E'_0 transition increases with increasing germanium concentration. This can be understood as the transitions $E'_0(1)$ and $E'_0(2)$ are split apart for larger x while they are not individually resolved, and as the transitions $E_1 + \Delta_1$ and E_0 merge with the E'_0 transition. Due to this superposition we find an evident deviation for the transition energy of the sample with 28.1% Ge concentration from the linear interpolation of the other samples, and for the sample with 27% Ge concentration the E'_0 transition is totally absent. Disregarding these two samples we obtain

$$E'_0(x) = [(3400 \pm 7) - (300 \pm 40)x] \text{ meV}, \quad (9)$$

which, according to the above discussion, must be considered as an average transition energy of $E'_0(1)$ and $E'_0(2)$.

For the p -type sample series we further resolve an unidentified transition in the main E'_0/E_1 structure. For this transition we obtain an energy

$$E_g = [(3504 \pm 25) + (353 \pm 116)x] \text{ meV}, \quad (10)$$

where we have used $n=2.5$ for fitting. Since the transition is very weak and obscured by other stronger structures, the energy expression given is relatively inaccurate. Interestingly, the value for $x=0$, $E_g=3504$ meV, is nearly identical with a critical point observed by Daunois *et al.* in pure silicon at 3500 meV.²² They showed using polarization-dependent measurements that this critical point is not consistent with a spin-orbit splitting of the E'_0 transition, but must be located elsewhere in the Brillouin zone.

The E_0 transition is very weak. Therefore, and because the E_0 structure merges with the E'_0/E_1 structure for higher germanium concentrations, we were not able to identify the E_0 transition in all spectra. The transitions $E_0(1)$ and $E_0(2)$ are too close for germanium concentrations up to 30% to be resolved individually (see Fig. 2). The transition $E_0 + \Delta_0$ could be identified only for the sample with 12.5% Ge concentration. The results for the E_0 transitions are summarized in Fig. 6. With the transition energy of pure silicon from Ref. 6 as a fix point we obtain

$$E_0(x) = [4175 - (2814 \pm 55)x] \text{ meV}, \quad (11)$$

where we have used $n=2.5$ for all fits. The measured transition energies are in good agreement with the values predicted by deformation potential theory for both, the E_0 transition and the $E_0 + \Delta_0$ transition of the sample with 12.5% Ge concentration. For the latter we have only a difference of 19 meV between experiment and theoretical calculation. The linear fit to the measured E_0 transition energies lies exactly between the theoretical curves of the $E_0(1)$ and $E_0(2)$ transition. We did not find any data for the E_0 transition in the literature.

The E_2 structure includes contributions from several critical points (Fig. 6). While we observe only one single transition in the n -type samples, there are two transitions in the p -type samples and a third transition in the sample with 12.5% Ge concentration. The twofold transitions can be

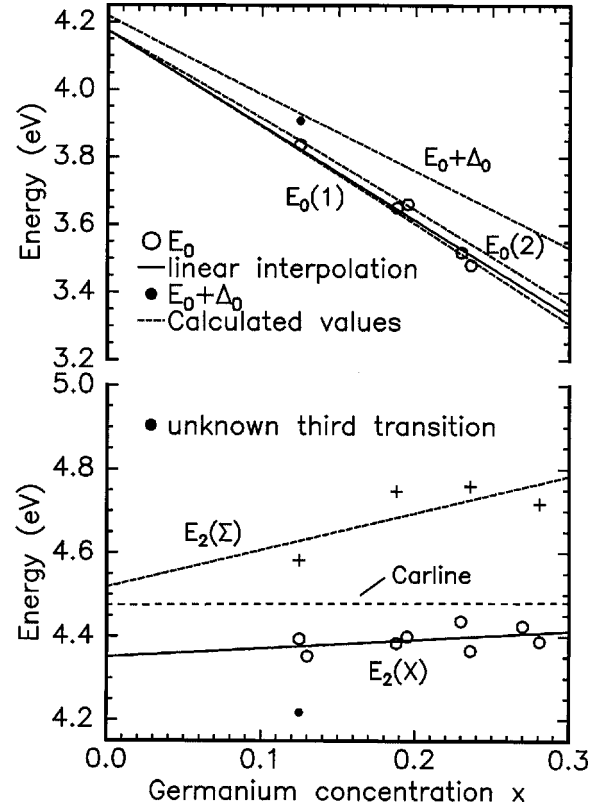


FIG. 6. Experimental ER results of strained $\text{Si}_{1-x}\text{Ge}_x$ at 70 K for transitions E_0 and E_2 . The data of the E_0 transition were linearly fitted including the energy 4.17 eV for pure silicon, $x=0$. Compared data of other work refers to Carline, Ref. 21.

identified with the critical points $E_2(X)$ and $E_2(\Sigma)$, while the third transition remains unexplained. Linear interpolation yields

$$E_2(X) = [(4351 \pm 38) + (210 \pm 180)x] \text{ meV} \quad (12)$$

$$E_2(\Sigma) = [(4518 \pm 129) + (880 \pm 600)x] \text{ meV}.$$

For $E_2(X)$ as well as for $E_2(\Sigma)$ we have used $n=3$ for a two-dimensional critical point. In contrast to all other critical points the E_2 transition energies become larger at increasing germanium concentration. In both expressions in Eq. (12) the uncertainty in the x dependent term is rather large; this leaves the possibility that the transition energies are constant, independent of the germanium concentration. By comparison to our results, the measurements by Carline for the E_2 transition appear to be a superposition of the transitions $E_2(X)$ and $E_2(\Sigma)$.

The E'_1 transition is very weak both in pure silicon and in pure germanium (see Ref. 13). In strained $\text{Si}_{1-x}\text{Ge}_x$, however, there is a relatively strong contribution of this critical point to the ER spectra. For the transition energy we obtain

$$E'_1(x) = [(5402 \pm 25) + (280 \pm 120)x] \text{ meV}, \quad (13)$$

where we have assumed a two-dimensional critical point ($n=3$). The E'_1 transition energy moderately increases at higher germanium concentration. Our extrapolation to $x=0$, $E'_1(0)=5402$ meV, is in good agreement with the value of 5375 meV given by Lautenschlager *et al.* for pure silicon at

82 K.²³ For three of the p -type samples we resolve another critical point at about 5750 meV, which might be a spin-orbit companion of the E'_1 transition. This energy is rather inaccurate as the structure appears close to the lower wavelength limit of our equipment.

For the p -type samples we have performed ER measurements in the temperature range from 10 to 300 K. The accuracy of the measurement is limited since the resolution for these measurements was lower than for those at 70 K, and the linewidths increase with increasing temperature. We have fitted the temperature dependence of all transitions to the phenomenological Varshni expression¹⁹

$$E(T) = \varepsilon_0 - \frac{\alpha T^2}{\beta + T} \quad (14)$$

and to the Viña formula¹⁰

$$E(T) = \varepsilon_B - \alpha_B \left[1 + \frac{2}{e^{\theta_B/T} - 1} \right]. \quad (15)$$

In both cases, the parameters in the expressions (14) and (15) determined from the experiments are on the same order of magnitude as for pure silicon and germanium. In general, all energies of critical points are expected to be subject to nonlinear variations when the alloy composition is changed from pure silicon to pure germanium. The reason is that even a linear change in the lattice constant (and thus strain) results in nonlinear energy shifts when entered into equations, where the deformation potential is composition dependent as

well. However, within the experimental error of our measurements, we did not observe any significant deviation of our experimental parameters in the Varshni or Viña expressions from these parameters linearly interpolated between Si and Ge. We note that the energy shift between 10 K and 300 K is about 160 meV for the E_0 transition and only about 30 meV for the E'_0 transition although both transitions have the same $\Gamma_{25'}$ VB state in common. A similar finding is well known from silicon and germanium: Transitions between bonding and antibonding p states have a much weaker temperature dependence than those between p and s states.

V. CONCLUSION

Using ER spectroscopy we have determined the transition energies of several critical points in strained $\text{Si}_{1-x}\text{Ge}_x$ layers for 12.5% $< x < 28.1\%$. Our experimental results for 70 K are in good agreement with theoretical calculations of strain shifts for the E_0 transition, while they deviate for the E_1 transition. The dependence of the transitions E'_0 , E_2 , and E'_1 on the germanium concentration is relatively weak. The intensity of the E_1 transition becomes smaller in strained material than that of the E'_0 transition, while the E'_1 transition becomes much stronger as compared to unstrained material. We have further reported the temperature dependence of the transition energies between 10 K and 300 K. The temperature dependent shifts of the transition energies are similar to those of pure silicon and germanium.

-
- ¹D. E. Aspnes, Surf. Sci. **37**, 418 (1973).
²A. Blacha, H. Presting, and M. Cardona, Phys. Status Solidi B **126**, 11 (1984).
³J. A. Vergés, D. Gltzel, M. Cardona, and O. K. Anderson, Phys. Status Solidi B **113**, 519 (1982).
⁴*Semiconductors. Physics of Group IV Elements and III-V Compounds*, edited by O. Madelung, Landolt-Börnstein, New Series, Group III, Vol. 17, Pt. a (Springer, Berlin, 1982), pp.63 and 105; *Semiconductors. Intrinsic Properties of Group IV Elements and III-V, II-V, and I-VII Compounds*, edited by O. Madelung, Landolt-Börnstein, New Series, Group III, Vol. 22, Pt. a (Springer, Berlin, 1987), p. 17.
⁵D. E. Aspnes and A. A. Studna, Solid State Commun. **11**, 1375 (1972).
⁶From Ref. 4 with an estimated energy shift of 10 meV between 10 and 70 K.
⁷Calculated with values from Y. P. Varshni, Physica (Amsterdam) **34**, 149 (1967).
⁸D. E. Aspnes, Phys. Rev. B **12**, 2297 (1975).
⁹G. E. Jellison and F. A. Modine, Phys. Rev. B **27**, 7466 (1983).
¹⁰L. Viña, S. Logothetidis, and M. Cardona, Phys. Rev. B **30**, 1979 (1984).
¹¹M. Chandrasekhar and F. H. Pollak, Phys. Rev. B **15**, 2127 (1977).
¹²F. H. Pollak and G. W. Rubloff, Phys. Rev. Lett. **29**, 789 (1972).
¹³C. Ulrich, Diploma thesis, Universitaet Ulm, Abt. Halbleiterphysik, 1994.
¹⁴Estimated value after M. Cardona, *Modulation Spectroscopy* (Academic Press, New York, 1969).
¹⁵M. L. Cohen and T. K. Bergstresser, Phys. Rev. **141**, 789 (1966).
¹⁶J. S. Kline, F. H. Pollak, and M. Cardona, Helv. Phys. Acta **41**, 968 (1968).
¹⁷T. P. Pearsall, F. H. Pollak, J. C. Bean, and R. Hull, Phys. Rev. B **33**, 6821 (1986).
¹⁸Y. Yin, F. H. Pollak, P. Auvray, D. Dutartre, R. Pantel, and J. A. Chroboczek, Thin Solid Films **222**, 85 (1992).
¹⁹Y. P. Varshni, Physica (Amsterdam) **34**, 149 (1967).
²⁰P. A. M. Rodrigues, M. A. Araújo Silva, F. Cerdeira, and J. C. Bean, Phys. Rev. B **48**, 18 024 (1993).
²¹R. T. Carline, C. Pickering, D. J. Robbins, W. Y. Leong, A. D. Pitt, and A. G. Cullis, Appl. Phys. Lett. **64**, 1114 (1993).
²²A. Daunois and D. E. Aspnes, Phys. Rev. B **18**, 1824 (1978).
²³P. Lautenschlager, M. Garriga, L. Viña, and M. Cardona, Phys. Rev. B **36**, 4821 (1987).